

Polarized light emission from GaInN light-emitting diodes embedded with subwavelength aluminum wire-grid polarizers

Ming Ma,¹ David S. Meyaard,² Qifeng Shan,³ Jaehee Cho,^{2,a)} E. Fred Schubert,² Gi Bum Kim,⁴ Min-Ho Kim,⁴ and Cheolsoo Sone⁴

¹*Future Chips Constellation, Department of Materials Science and Engineering, Rensselaer Polytechnic Institute, Troy, New York 12180, USA*

²*Future Chips Constellation, Department of Electrical, Computer, and Systems Engineering, Rensselaer Polytechnic Institute, Troy, New York 12180, USA*

³*Future Chips Constellation, Department of Physics, Applied Physics and Astronomy, Rensselaer Polytechnic Institute, Troy, New York 12180, USA*

⁴*Advanced Development Group, LED Business, Samsung Electronics, Yongin 446-920, Korea*

(Received 31 May 2012; accepted 26 July 2012; published online 6 August 2012)

We demonstrate a back-emitting (sapphire-substrate emitting) linearly polarized GaInN light-emitting diode (LED) embedded with a subwavelength-sized aluminum wire-grid polarizer (WGP). Rigorous coupled wave analysis is implemented to study the polarization characteristics of such a WGP LED. The aluminum nanowire grating with a period of 150 nm is located on the sapphire backside of a GaInN LED structure and is fabricated by electron-beam lithography and inductively coupled plasma reactive-ion etching. A polarization ratio of 0.96 is demonstrated for a WGP GaInN LED in good agreement with simulation results. © 2012 American Institute of Physics. [<http://dx.doi.org/10.1063/1.4744422>]

The high efficiency of light-emitting diodes (LEDs) already provides very substantial energy savings in a number of lighting applications.^{1–3} Moreover, LEDs fundamentally offer new functionalities such as the control of color temperature, dimming level, pulsation, far-field emission pattern, and even polarization, all of which is far less controllable for traditional lighting sources.⁴ Such optically functional light sources (i.e., LEDs) can provide many benefits in general lighting, automobiles, and display applications.^{5,6} However, the control of one property—optical polarization—still remains insufficient, despite the fact that LEDs with polarized emission would be extremely useful particularly for liquid-crystal display (LCD) backlighting and projection-display lighting, as well as for sensing and communication applications. For example, in a LCD, only polarized emission can be switched on and off. Currently backlighting sources emit unpolarized light and absorptive polarizers are separated from the LED backlighting unit, which results in a loss of light.⁷ Therefore, if a LED can generate polarized emission with high efficiency, it will undoubtedly be beneficial to the energy efficiency of LCDs.⁸ Previously it has been reported that the light emitted from GaInN LEDs epitaxially grown on different crystal planes of sapphire substrates shows some degree of polarization.^{9–11} However, the polarization ratios (PRs) were not high enough for practical applications. In the present study, we investigate polarized emission from a GaInN LED in which a subwavelength aluminum wire-grid polarizer is embedded.

A wire-grid polarizer (WGP) relies on a conductive metal grating and its interaction with the incident light, particularly its electric field component. Embedding a metallic WGP on top of a LED (which will be denoted as a “WGP LED”) offers several advantages: First, an extremely high

PR is possible with a WGP structure. Second, a WGP LED allows for the light with the undesired polarization to be reflected back (i.e., not absorbed), where it may be scattered at the *p*-type metal contact and thus, by means of a scattering event, have another chance to assume the polarization that is transmitted through the polarizer.¹² In order to optimize the parameters of the grating, rigorous coupled wave analysis (RCWA) is implemented in MATLAB.^{13,14} In this method, Maxwell’s equations are solved in three regions: the substrate, grating, and the ambient. Separate equations are considered and solved for the transverse electric (TE) and the transverse magnetic (TM) mode light. Here, the TE mode light is defined as light whose electric field component oscillates along the direction perpendicular to the plane of incidence; and the TM mode light is defined as light whose magnetic field component oscillates along the direction perpendicular to the plane of incidence. The incident light is assumed to emit uniformly from a planar, randomly polarized light source, similar to the real case of a LED. The equations introduced in this paper are relevant to the TE mode; for the TM mode, a similar derivation can be performed. A complete derivation of equations and methods of solution for both modes of light is found in the literature.¹² Figure 1 shows the geometry defined for this work, as well as the optimization parameters of interest.

To simplify the theoretical simulation, the area of the polarizer is assumed to be infinitely large. For visible-light applications, The WGP will have several thousand periods per centimeter, so this assumption is justified. In order to solve Maxwell’s equations, the electric field in each of the three regions of interest should be first described. If we define the interface of the grating region to lie in the *y* plane and consider the light to be a plane wave, we can generalize any incident light in terms of its *x* and *z* components, as shown in Fig. 1. We define the incident light in terms of its electric field components

^{a)}choj6@rpi.edu.

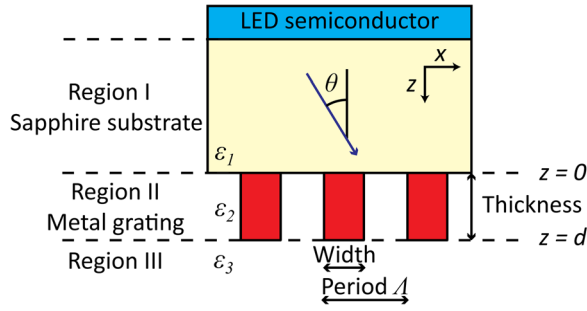


FIG. 1. Schematic diagram of the simulated grating geometry, showing the xz coordinate system used, as well as the important parameters to be optimized.

$$E_{incident} = \exp[-j(k_{x,0}x + k_{z,0}z)], \quad (1)$$

where $k_{x,0}$ and $k_{z,0}$ are the 0th order wave vector in the x and z directions, respectively, and j is the imaginary number ($j^2 = -1$). When the incident wave reaches the grating, a set of waves will be reflected backwards. We can then express the electric field in region I as a sum of the incident and all reflected waves

$$E_I = \exp[-j(k_{x,0}x + k_{z,0}z)] + \sum_i R_i \exp[-j(k_{x,i}x + k_{z,i}z)], \quad (2)$$

where R_i is the amplitude of the i th order reflected wave, $k_{x,i}$ refers to the i th order wave vector in the x direction in region I, and $k_{z,i}$ refers to the i th order wave vector in the z direction in region I.

The periodic grating, located in region II, is assumed to consist of two materials, in this case, metal and air. We can then express the electric field in the grating in terms of its complex field components. This is implemented in the equation

$$E_{II} = \sum_i S_i(z) \exp[-j(k_{x,i}x + k_{z,0}z)], \quad (3)$$

where S_i is the normalized amplitude of the i th space harmonic field. For the grating region, we discretize parameters such as complex permittivity, $\varepsilon(x)$, by expressing them as a sum of Fourier components

$$\varepsilon(x) = \sum_p \varepsilon_p \exp(jKpx), \quad (4)$$

where ε_p is the p th Fourier component of the relative permittivity in the grating region, and Λ is the grating period with $K = \frac{2\pi}{\Lambda}$.

In region III, there are no reflected waves, but simply the sum of waves transmitted through the grating

$$E_{III,y} = \sum_i T_i \exp[-j(k_{x,i}x + k_{z,i}(z-d))], \quad (5)$$

where T_i is the amplitude of the i th order transmitted wave and d is the thickness of the grating. After defining the electric field in each region, we solve the Maxwell-Faraday equation in all areas of interest, resulting in a series of coupled differential equations. Using the known electrostatic boundary conditions, such as continuous tangential E and H at the boundary interfaces ($z=0$ and $z=d$), we can solve for the transmitted and reflected waves. Here, we define the polarization ratio, PR , as

$$PR = \frac{|I_{TE} - I_{TM}|}{I_{TE} + I_{TM}}. \quad (6)$$

That is, unpolarized light ($I_{TE} = I_{TM}$) and highly polarized light ($I_{TM} \gg I_{TE}$) has a polarization ratio of zero and about one, respectively. Using this calculation method, we can compare the effect of all relevant parameters such as choice of metal, metal-film thickness, metal-stripe width, and grating period. We optimize these parameters for maximum transmitted TM intensity, as well as maximum polarization ratio.

First we compare different choices of grating material. Each different metal can be simulated by including its complex permittivity in the grating region. In this manner, effects such as absorption and reflection can be accurately included in this model. Intuitively, we expect that a metal with high conductivity would be a good choice. Comparing the simulated results using various thicknesses and periods for silver, gold, and aluminum (Al) gratings, Al exhibits best overall performance.¹² There is an inherent trade-off between increasing the metal-stripe width to increase the polarization ratio, and maintaining a very high transmitted intensity. Figures 2(a) and 2(b) shows the simulated polarization ratio and transmitted TM mode intensity ratio for an Al grating with a 150 nm period, respectively. Here, the transmitted TM mode intensity ratio is defined as the ratio between the transmitted TM mode intensity and the incident TM mode intensity. A transmitted TM mode intensity ratio of 1 means all of the

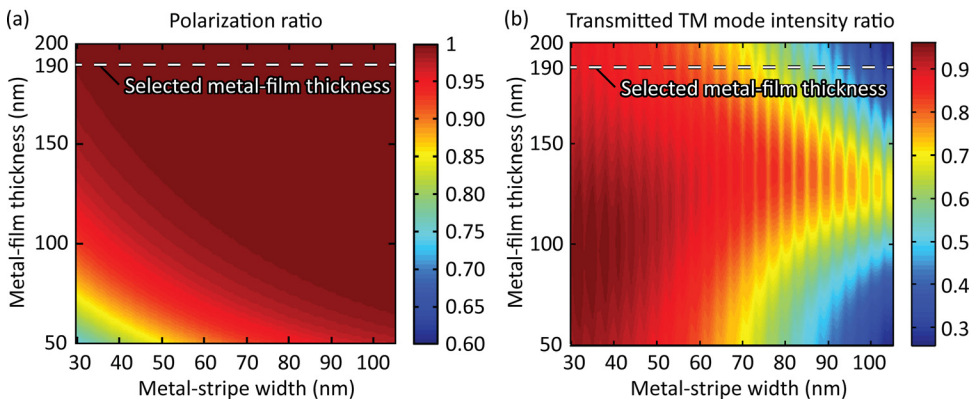


FIG. 2. Simulated (a) polarization ratio and (b) transmitted TM mode intensity ratio, using a fixed 150 nm period Al WGP, as a function of the metal-stripe width and the metal-film thickness. The dashed line indicates the 190 nm metal-film thickness selected for fabrication.

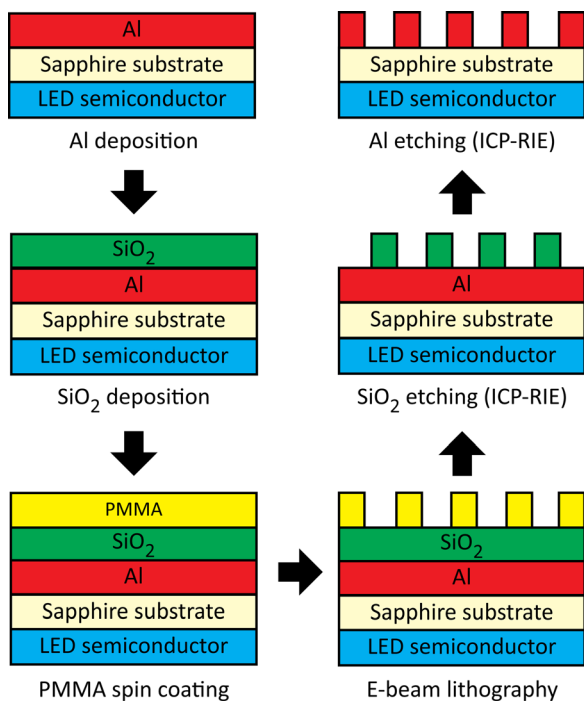


FIG. 3. Schematic diagram of the process flow for the fabrication of the Al WGP LED.

incident TM mode light is transmitted through the WGP. The period of 150 nm is chosen in consideration for the limitations of the available electron-beam lithography system. As the metal-film thickness of the grating is increased, the polarization ratio increases, but at the cost of transmitted intensity. Based on the simulation results, a grating with a metal-film thickness of 190 nm is chosen; it has high polarization ratio over a large range of the metal-stripe widths.

GaN LEDs emitting at 460 nm are grown on a double-side-polished (0001) oriented c-plane sapphire substrate by using a single-wafer metalorganic vapor phase epitaxy

(MOVPE) system. Mesa devices with $300 \times 300 \mu\text{m}^2$ chip area are fabricated under a standard LED fabrication process, followed by the depositions of reflecting *n*-type metal contacts (Ti/Al—30/250 nm) and *p*-type metal contacts (NiZn/Ag—5/200 nm). After that, the Al WGP is fabricated on the backside of the fabricated LEDs. The process flow for the fabrication of the Al WGP is schematically shown in Fig. 3. At first, an Al layer with a thickness of about 190 nm is deposited on the backside of the sapphire of the fabricated LEDs by using electron-beam evaporation. This is followed by electron-beam deposition of a layer of SiO₂ with a thickness of about 40 nm. Subsequently, a layer of the poly methylmethacrylate (PMMA) electroresist is spin-coated onto the SiO₂ layer. The SiO₂ is used as a hard mask to etch Al due to the poor etch resistivity of the electroresist.¹⁵ The PMMA is patterned by using electron-beam lithography to define a grating array within an area of $300 \times 300 \mu\text{m}^2$. The patterned resist has a period of 150 nm and a resist linewidth of about 75 nm, as shown in Fig. 4(a). The grating pattern is then replicated into the underlying SiO₂ layer through a fluorine-based inductively coupled plasma reactive-ion etching (ICP-RIE) process. The SiO₂ layer is etched under 300 W ICP power and 100 W RIE power with 15 sccm of CHF₃ at 10 mTorr to form the SiO₂ hard mask. The patterned SiO₂ has a period of 150 nm and a SiO₂ linewidth of about 90 nm, as shown in Fig. 4(b). Finally, the Al layer is etched through a chlorine-based ICP-RIE process by using the patterned SiO₂ as a hard mask. The Al layer is etched under 400 W ICP power and 75 W RIE power with 30 sccm of BCl₃ and 10 sccm of Cl₂ at 5 mTorr. The Al nanowire gratings have a period of 150 nm and an Al linewidth of about 100 nm, as shown in Fig. 4(c).

To measure the polarization ratio of the light emission from such a WGP LED, a rotating linear polarizer is placed between the GaInN WGP LED and a Si photo-detector, as illustrated in Fig. 5(a). The different polarizations of light are detected by rotating the linear polarizer in line with the

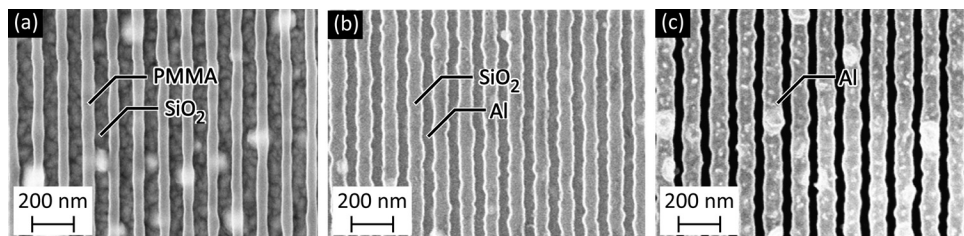


FIG. 4. Scanning electron microscopy (SEM) images of (a) patterned PMMA on top of the SiO₂ layer; (b) patterned SiO₂ on top of the Al layer; and (c) Al WGP on top of the sapphire substrate. The gratings have a period of 150 nm.

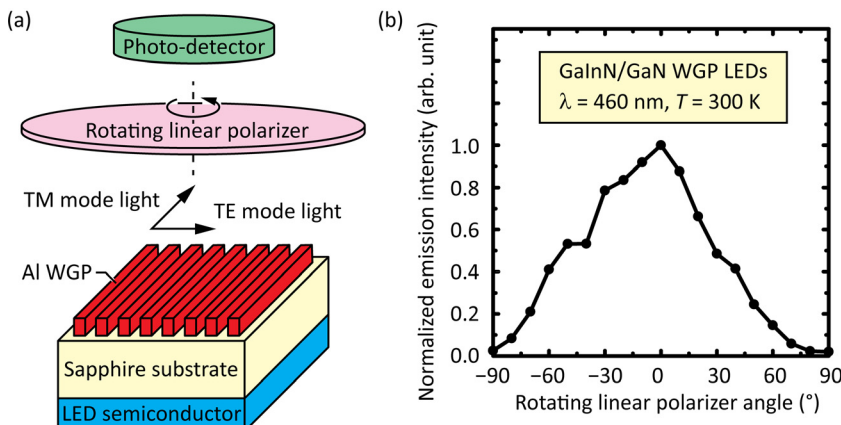


FIG. 5. (a) Schematic illustration of the measurement setup; (b) measured EL intensity of the WGP LED as a function of the orientation angle of a rotating linear polarizer.

designed direction of polarization. We confirmed that a LED without a WGP shows completely unpolarized emission. Figure 5(b) shows the electroluminescence (EL) intensity of the WGP LED as a function of the orientation angle of the rotating linear polarizer. As shown in Fig. 5(b), the measured intensity varies with the polarizer-rotating angle, revealing polarized light emission from the WGP LED. The maximum and minimum intensities indicate the relative magnitude of the TM mode light and TE mode light, respectively. The measured intensity of the TM mode light is about 50 times greater than the intensity of the TE mode light, corresponding to a polarization ratio of about 0.96. Note that our approach allows for an Al WGP with good uniformity and surface coverage since it is fabricated on the backside of the LED, thus, resulting in a high polarization ratio.

In summary, a back-emitting (sapphire-substrate emitting) linearly polarized GaInN LED emitting at 460 nm with an embedded subwavelength-sized Al WGP is demonstrated. Rigorous coupled wave analysis is implemented to study and optimize the polarization characteristics of such a WGP LED. An optimized Al nanowire grating with a period of 150 nm is fabricated on the sapphire backside of a GaInN LED structure by electron-beam lithography and ICP-RIE. A polarization ratio of 0.96 is experimentally demonstrated for a GaInN LED. The polarization ratio of 0.96 is consistent with the simulation results based on rigorous coupled wave analysis. The results open the door for practical applications of polarized LEDs.

The authors gratefully acknowledge support by Samsung Electronics, Korean Ministry of Knowledge Economy and Korea Institute for Advancement of Technology through International Collaborative R&D Program, the National Sci-

ence Foundation, Sandia National Laboratories, Department of Energy, Magnolia Optical Technologies, and the National Research Foundation of Korea Grant funded by the Korean Government (MEST) (NRF-2011-220-D00064). Authors D.S.M., J.C., and E.F.S. were supported by Sandia's Solid-State Lighting Sciences Center, an Energy Frontier Research Center funded by the U. S. Department of Energy, Office of Basic Energy Sciences.

¹N. Horiuchi, *Nat. Photonics* **4**, 738 (2010).

²J. H. Burroughes, D. D. C. Bradley, A. R. Brown, R. N. Marks, K. Mackay, R. H. Friend, P. L. Burns, and A. B. Holmes, *Nature* **347**, 539 (1990).

³E. F. Schubert, *Light Emitting Diodes*, 2nd ed. (Cambridge University Press, Cambridge, 2006).

⁴E. F. Schubert and J. K. Kim, *Science* **308**, 1274 (2005).

⁵M. R. Krames, O. B. Shchekin, R. Mueller-Mach, G. O. Mueller, L. Zhou, G. Harbers, and M. G. Craford, *J. Disp. Technol.* **3**, 160 (2007).

⁶J. Shakya, K. Knabe, K. H. Kim, J. Li, J. Y. Lin, and H. X. Jiang, *Appl. Phys. Lett.* **86**, 091107 (2005).

⁷P. Yeh and C. Gu, *Optics of Liquid Crystal Displays* (Wiley, New York, 2010).

⁸L. Zhang, J. H. Teng, S. J. Chua, and E. A. Fitzgerald, *Appl. Phys. Lett.* **95**, 261110 (2009).

⁹H. Masui, A. Chakraborty, B. A. Haskell, U. K. Mishra, J. S. Speck, S. Nakamura, and S. P. DenBaars, *Jpn. J. Appl. Phys., Part 1* **44**, 1329 (2005).

¹⁰M. F. Schubert, S. Chhajed, J. K. Kim, E. F. Schubert, and J. Cho, *Appl. Phys. Lett.* **91**, 051117 (2007).

¹¹M. Ueda, M. Funato, K. Kojima, Y. Kawakami, Y. Narukawa, and T. Mukai, *Phys. Rev. B* **78**, 233303 (2008).

¹²D. S. Meyaard, *Master's thesis*, Rensselaer Polytechnic Institute, 2009.

¹³M. G. Moharam and T. K. Gaylord, *J. Opt. Soc. Am.* **71**, 811 (1981).

¹⁴M. G. Moharam, E. B. Grann, D. A. Pomet, and T. K. Gaylord, *J. Opt. Soc. Am. A* **12**, 1068 (1995).

¹⁵J. J. Wang, F. Walters, X. Liu, P. Sciortino, and X. Deng, *Appl. Phys. Lett.* **90**, 061104 (2007).